Measurement 106 (2017) 283–290

Contents lists available at ScienceDirect

Measurement

journal homepage: www.elsevier.com/locate/measurement

# Characterization of thermoelectric generator for energy harvesting

C.L. Izidoro [a], O.H. Ando Junior [b,*], J.P. Carmo [c], L. Schaeffer [d]

[a] Beneficent Association of Santa Catarina Coal Industry, Brazil
[b] UNILA – Federal University of Latin American Integration, Brazil
[c] USP, University of São Paulo, Brazil
[d] UFRGS, Federal University of Rio Grande do Sul, Brazil

ARTICLE INFO

*Article history:*
Available online 8 January 2016

*Keywords:*
Thermoelectric generator (TEG)
Power source characterization
Energy harvesting
Acquisition data system
Cogeneration

ABSTRACT

This paper presents a system for characterization of thermoelectric generators (TEGs) for energy harvesting. This system can monitor and characterize up to three TEGs simultaneously and it is comprised by two main electronic circuits: The first one is composed by twelve input channels being three for reading voltage, three for reading current by making use of instrumentation amplifiers (reference ACS712) and six thermocouples for signal reading (<400 °C). The second electronic circuit consists of a proportional–integral–derivative (PID) controller with two pulse width modulation (PWM) input channels for controlling the heat (thermoresistance) and cooling (controlled cooler) sources respectively, following a pre-defined temperature gradient. The TEG measured data for the voltage, current and temperature can be acquired in real-time with development in Delphi® language and displayed through both a numeric and graphical display. In order to validate the precision and accuracy two commercial TEG modules (reference inbC1-127.08HTS) compatible with temperatures up to 200 °C without signal degradation were used in series. The acquisition system resulted in a precision of ±5%, ±2% and ±1.5% for the temperature, voltage and current respectively, with a maximum error value of 1%. Its possible utilizing this acquisition system acquire data from TEG obtain graphics response and determinate some characteristics how internal resistance, open circuit voltage, power output and temperatures gradient form any conditions of operation. All of these features combined with the low-cost under R$973.80 (≈324.43 €) makes this system suitable for a wide range of applications for standalone power system or heat recycling systems for cogeneration of electricity. Knowledge of the electrical characteristics of TEGs is of great interest in co-generation systems to design the same in order to achieve the best possible performance.



## 1. Introduction

The use of modern technologies and new energy sources generated changes in human life providing not only increased economic productivity but also to an improved quality of life [1]. According to Camacho-Medina et al., it is estimated that by 2035 the world energy consumption will increase by around 40%, which leads to the search for new technologies of generation [2].

One of the alternative technologies is the search for sources that allow increasing the supply of energy in a sustainable way [3,4].

In this context comes the solid-state generator as a promising alternative that based on Seebeck effect of thermoelectric materials enabling the conversion of thermal energy into electrical energy [5,6]. With the use of solid state generators is possible generate clean energy for energy harvesting in a simple and reliable way, with advantages of no moving parts, low complexity, silent operation, low maintenance cost and no environment impact [7]. Because they are solid state devices that operate in extreme conditions, a temperature gradient is necessary to generate power with an energy efficiency of 5–15% which is considered good [8,9].

In this context, an integrated data acquisition system (hardware and software) for monitoring TEG is presents in this paper. The thermal part of the process consists of a heating and cooling system capable of generating a temperature gradient, this system is controlled by a microprocessor. The acquisition system is set to make the temperature reading of the high temperature surface and the low temperature surface of the thermoelectric material in addition to the voltage and generated power. The software displays graphically the readings of the experiment showing the performance curves. Lastly, the system validation and the characterization of TEG are presented.

* Corresponding author.
*E-mail addresses:* cleber.izidoro@satc.edu.br (C.L. Izidoro), oswaldo.junior@unila.edu.br (O.H. Ando Junior), jcarmo@sc.usp.br (J.P. Carmo), schaefer@ufrgs.br (L. Schaeffer).

http://dx.doi.org/10.1016/j.measurement.2016.01.010
0263-2241/

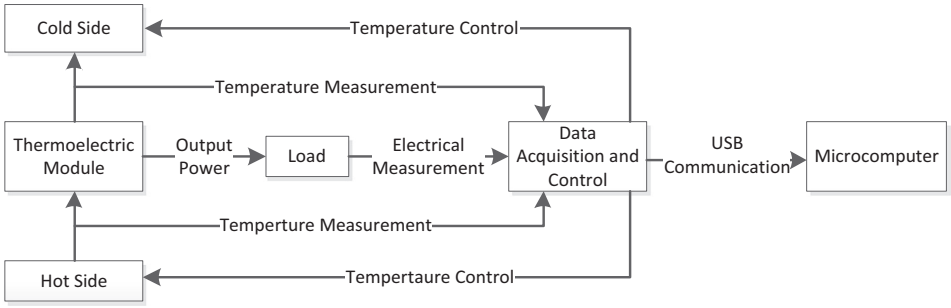


**Fig. 1.** Acquisition system diagram.

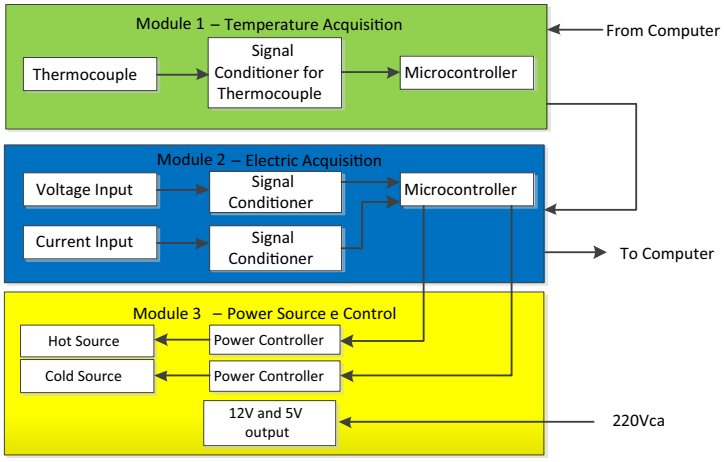


**Fig. 2.** Schematic's hardware structure.

## 2. System architecture

The complete system architecture, involving heating, cooling and data acquisition is shown in Fig. 1. This architecture is the continuation of a work described in an earlier paper [10].

This system is a second hardware developed, because, in the previous version, the physical structure presented some problems during its manufacture and test. For example, when some adjustments during the tests were required, the closed box with top access difficult it. Several loose wires difficult the maintenance process too. Therefore, we develop a new manufacturing model, with a modular structure, where the boards can even be exchanged place if necessary, without any additional configuration change.

Another improvement made was the inclusion of electronic circuits with better accuracy, how to the MAX31855 for temperature, and the ACS712-5 for current acquisition, beyond, the change of microcontroller, the PIC16F877A with 20 MHz clock to the PIC18F452 with 40 MHz clock. Especially in the temperature reading, the time of conversion was reduced by about 20 ms to about 5 ms. Further changes were made in the firmware of the microcontroller in order to improve the accuracy of readings with a reading performed at each 50 ms approximately. All reading and temperature adjustment elements are controlled by microprocessor-based systems, they communicate through a USB port on the PC, where you can see the system diagram, as shown in Fig. 1.

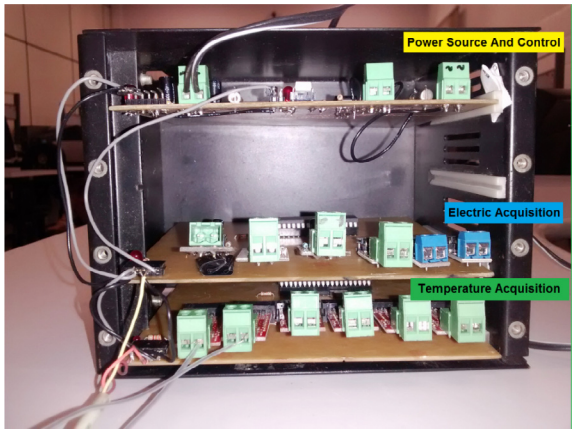


**Fig. 3.** Acquisition system structure.

### 2.1. Hardware configuration

The decentralized hardware system divided into 3 modules, shown in Fig. 2, facilitates the interconnection of the elements needed for the testing. The module 1, represented in green has thermocouples and signal conditioners. The module 2 is the electrical signals acquisition system, represented in blue[1], responsible for adjust voltage and electric current. Finally, the module 3, shown in yellow, makes the power load control, in addition to having the power source of 5–12 $V_{dc}$ to all systems.

In Fig. 3 the modular acquisition system is shown, where the upper module has the DC power supply and temperature control.

[1] For interpretation of color in Figs. 2 and 4, the reader is referred to the web version of this article.

The module in the middle has three voltage channels and three current channels. The bottom module has other six channels for temperature measurement.

### 2.2. Calibration

A calibration is performed for all channels to ensure accuracy of the readings due to possible of non-linearity when compared to a calibrated device.

Initially, the temperature curves were generated in a range from 1 °C to 125 °C, with steps of 2 °C, until reaching the temperature limit. The results are shown in Fig. 4, the curve generated with a calibrated instrument is blue, the temperature read by the bench without calibration is red, and the error is shown in green. The error reaches up to 12% without calibration.

Through the data collected, was generated a linear function, described in (1), and this inserted in data acquisition software developed in order to minimize the error. After the corrections and linearization, the maximum error generated was 5% and the minimum around 0.8%. In the graph of Fig. 5, the trend line applied to fitting curve shows the correlation of the reference curve, the *R* square function shows a value of 0.984, implying a great relationship between the reference curve and that adjusted in software.

$$Y = [(0.9879X) - 0.1936] \quad (1)$$

Similarly, the electrical current calibration was performed; the measures do from 0 to 5 A in steps of 0.25 A. The linearization and calibration curve are shown in Fig. 6, where the maximum error of the curve without adjustment is around 4%.

Applying the linearization of the equation, the error decreased to around ±1.5% for the entire application range with the generated Eq. (2). Likewise, in accordance with Fig. 7, correlation and trend curve applied lead to a correlation value of 0.999.

$$y = [(0.9869x) - 0.0128] \quad (2)$$

For the voltage, the maximum measurement value is 24 V, the adjustment carried out in a range of 0.5–0.5 V, as shown in Fig. 8, where the error exceed 5%.

After applying the linearization technique, the error was found to decrease to less than 2%, as shown in Fig. 8, producing the Eq. (3), and the correlation value between the two values was approximately 1 (see Fig. 9).

$$Y = [(0.9988x) - 0.0719] \quad (3)$$

### 2.3. Software structure

Connected to the microprocessor acquisition system software, via a USB communication cable, a software developed in visual platform using Borland Delphi 7.0® is responsible for showing in graphs all data acquired simultaneously. In Fig. 10 is shown a group of graph generated by the acquisition system. The first graph shows the temperature of the high temperature side in blue and low temperature side temperature in black.

In other graphics are shown the voltage, the current and the power generated, as shown in Fig. 10a. In Fig. 10b, you can view data instantly and numerically.

These data are saved in text files individually for each channel and can be treated after using commercial software.

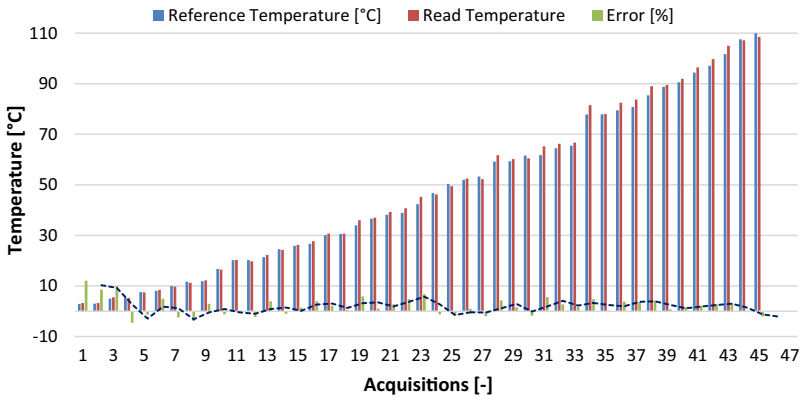


**Fig. 4.** Temperature curve without adjustment.

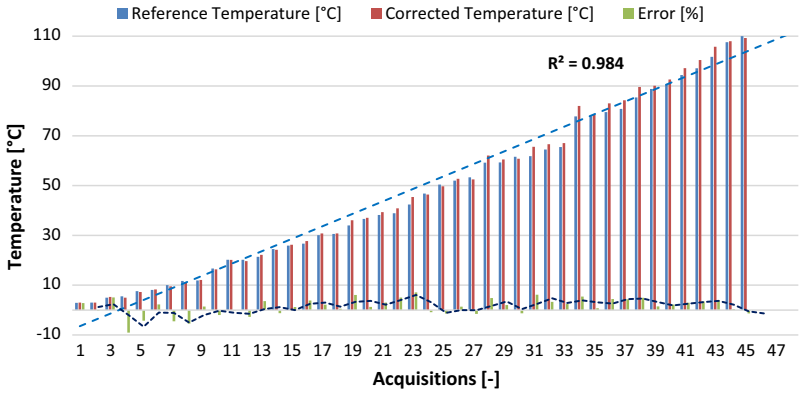


**Fig. 5.** Temperature curve with adjustment.

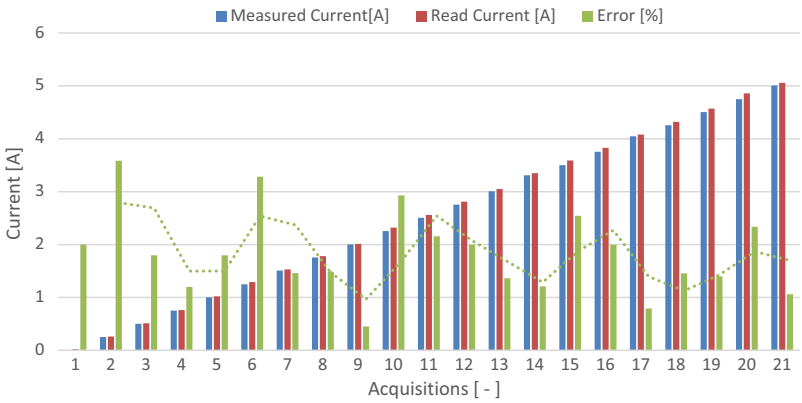


**Fig. 6.** Current curve without adjustment.

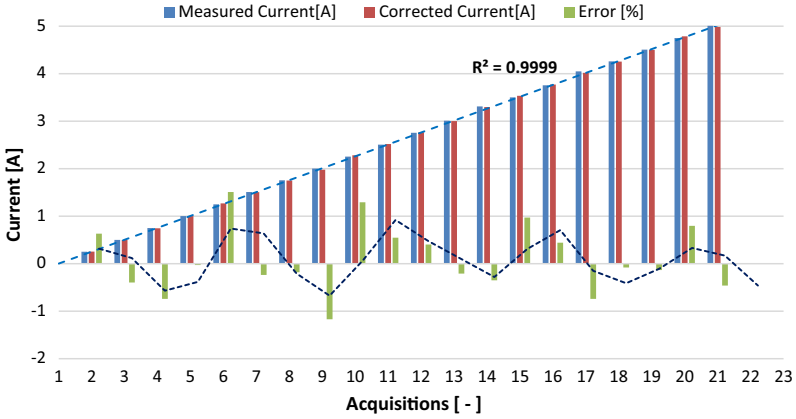


**Fig. 7.** Current curve with adjustment.

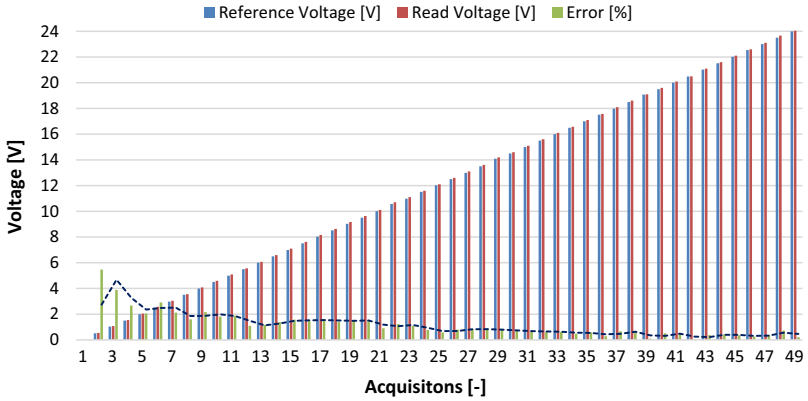


**Fig. 8.** Voltage curve without adjustment.

## 3. System architecture

To perform the characterization system, external devices was employed to obtain the correct temperature gradients. As heat source for heating the element was used an electric heating resistors that can reach up to 1500 W of power, and for cooling a heat sink made of aluminum with a fan to keep stable the temperature.

In Fig. 10a, the diagram experiment blocks is shown, and in the Fig. 10b, the experiment being carried out is shown. To assemble the experiment, the heating system is placed at the bottom, on it an aluminum plate with small holes for insertion of thermocouples, on this board is inserted the thermoelectric module inbC1-127.08HTS model, following a second well drilled aluminum plate for insertion of thermocouples is put on, and finally the heat sink and the fan to remove heat are put on top. In order to provide an electrical load, power resistors have been connected to their output terminals. The respective modules of the data acquisition system measure the generated voltage and electric current.

Two electronics boards equipped with microcontroller PIC18F452 at 40 MHz of clock are responsible for data analog acquisition and control of outputs. To acquire temperature, thermocouples type K was utilized coupled in MAX31855 cold junction

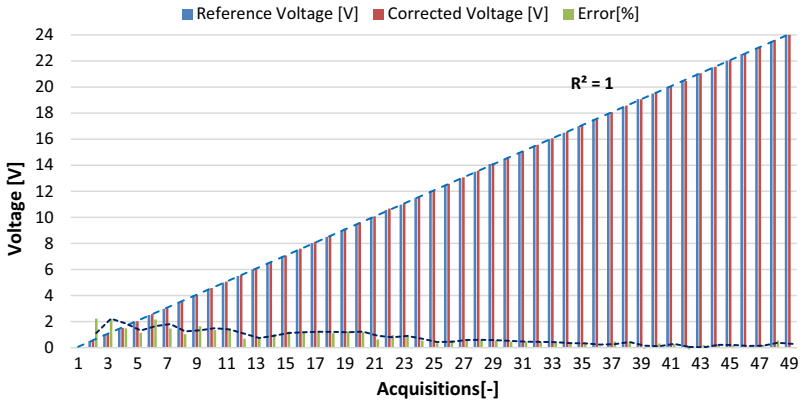


**Fig. 9.** Voltage curve with adjustment.

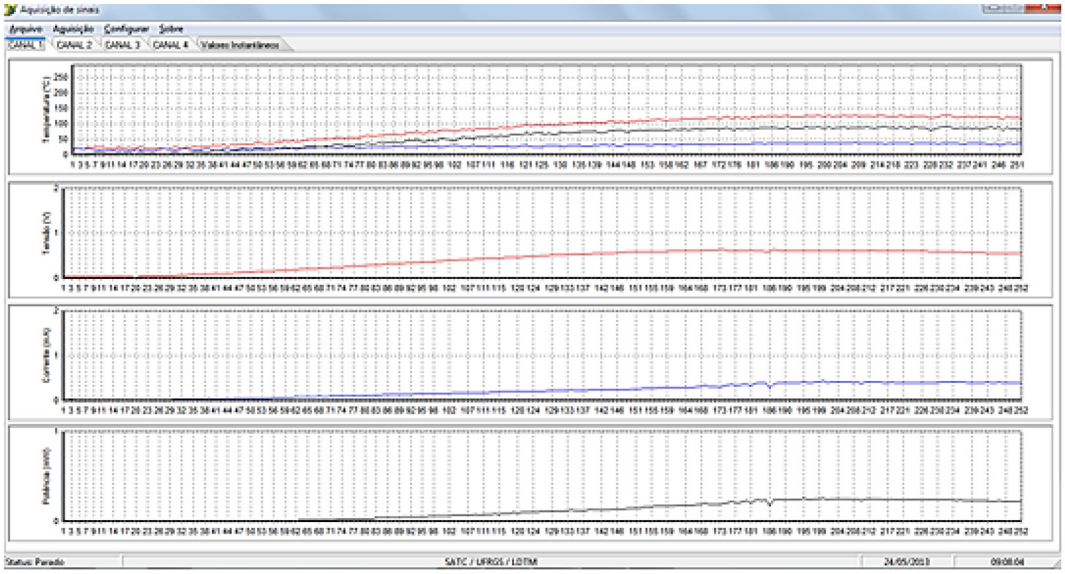

(a)

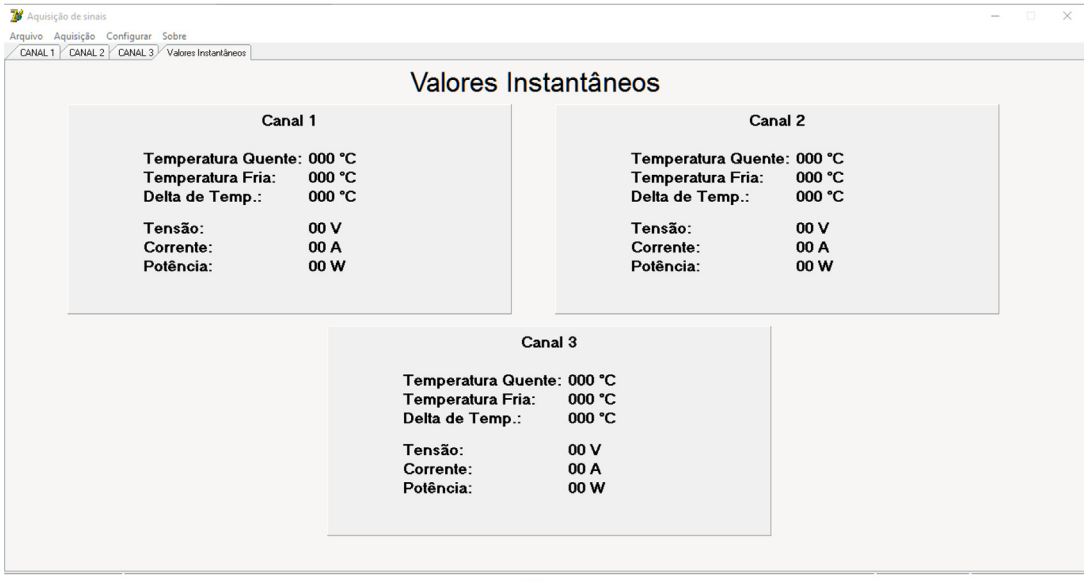


(b)

**Fig. 10.** Acquisition software.

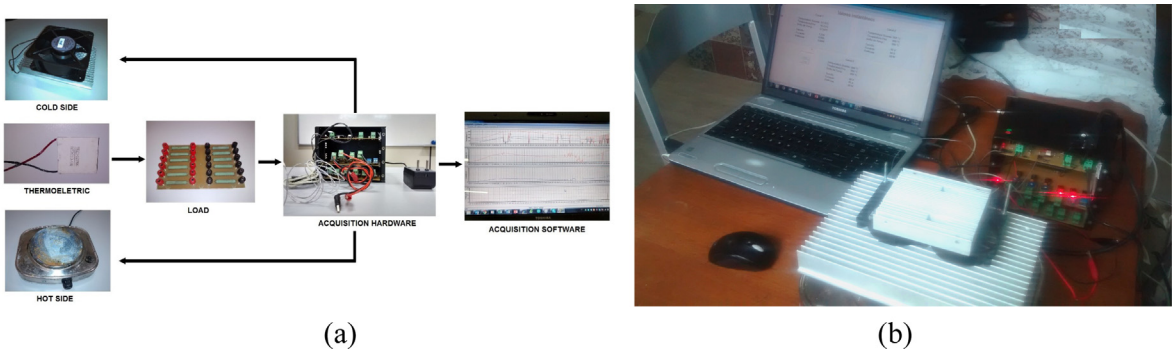


**Fig. 11.** Diagram system mounting blocks (a) and assembled experiment (b).

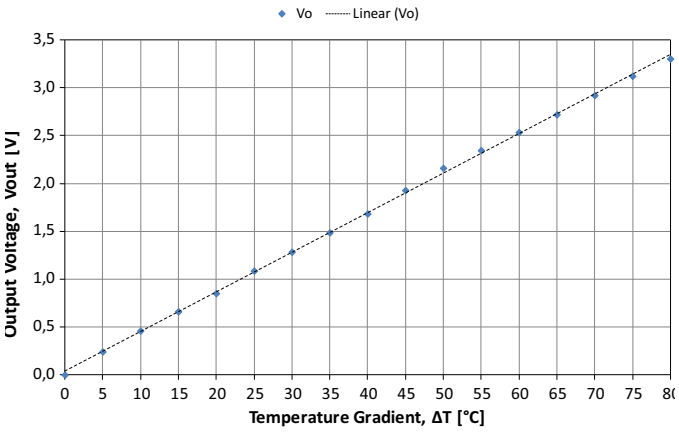


**Fig. 12.** The open-circuit voltage, $V_{out}$ [V], as function of the temperature gradient, $\Delta T$ [°C].

compensated thermocouple to digital converter, for current the ACS712-5 was utilized, permitting reads up 5 A, and for voltage, a voltage divisor was develop for reads up 24 Vcc. To computer communication, a proprietary protocol utilized, through USB to Serial converter de data transmitted.

The output temperature control effected by PWM (Pulse Width Modulation) with a power electronic circuit, in AC for the heat and DC for the cold. In order to perform the experiment correctly, the software starts simultaneously reading the sensors and controlling the power loads until the gradient reached generating the curves that will be described later. The acquisition is performed at an interval of 100 ms for each data, temperature of the high temperature source, temperature of the low temperature source, voltage and electric current. Internally, the data acquisition software determines the electrical power generated by temperature gradient result.

## 4. Results

In this section, the results from tests for characterization and validation of a inbC1-127.08HTS module are presented. The open circuit test is to determine the increase of the output voltage ($V_{out}$) open for different gradients ($DT$). In Fig. 12 is shown the graph obtained from the results of the open circuit test.

Based on the data shown in Fig. 11, it's possible observe that the generated voltage constantly varies with the temperature gradient. Applying the method of least squares for all output voltage samples ($V_{out}$), we obtain the following equation for the open circuit voltage: ($V_{out} = 41{,}2815 \times \Delta T$ [mV]). By comparing the sampled values with the trend line, in all samples the $V/I$ are proportional, in other words, the internal resistance of the thermoelectric module is constant with temperature test. Thus, the internal resistance of the entire TEG (Fig. 13a) can be determine from values of the internal resistance of the samples ($R_{int}$) measured in [Ω] to different temperature gradients ($\Delta T$). A statistical analysis of the samples internal resistance ($R_{int}$) measured in the tests was made [Ω], the average of the internal resistance ($R_{int}$) was calculated to different temperature gradients ($\Delta T$) and their standard deviations ($\sigma_n$) determined. Then, we calculated the average internal resistance ($R_{int\_média}$) of all samples and obtained their respective standard deviation sample set ($\sigma_{médio}$). It is noteworthy that in

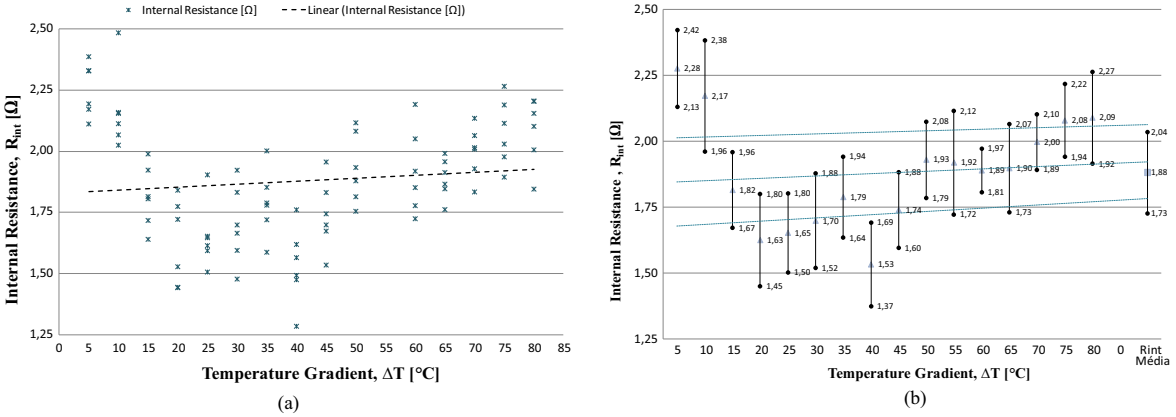


**Fig. 13.** (a) The internal resistance of TEG, $R_{int}$ [Ω], as function of the temperature gradient, $\Delta T$ [°C]. (b) The medium and standard deviation values of the internal resistance of TEG, $R_{int}$ [Ω], as function of the temperature gradient, $\Delta T$ [°C].

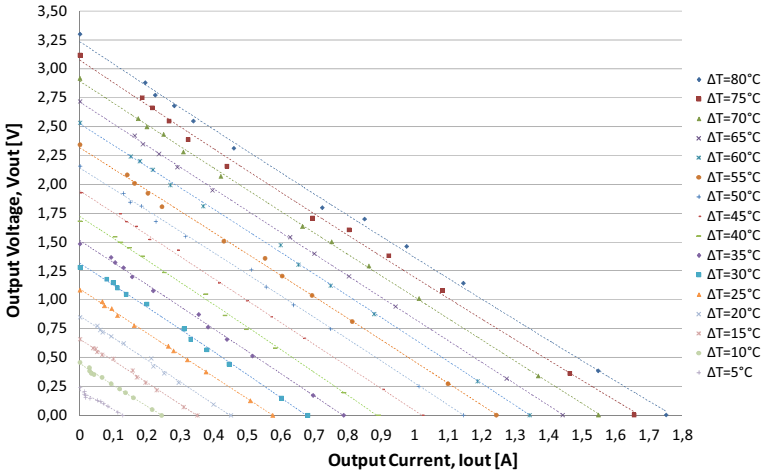


**Fig. 14.** The output voltage, $V_{out}$ [V] versus the output current, $I_{out}$ [A], for different temperature gradient, $\Delta T$ [°C].

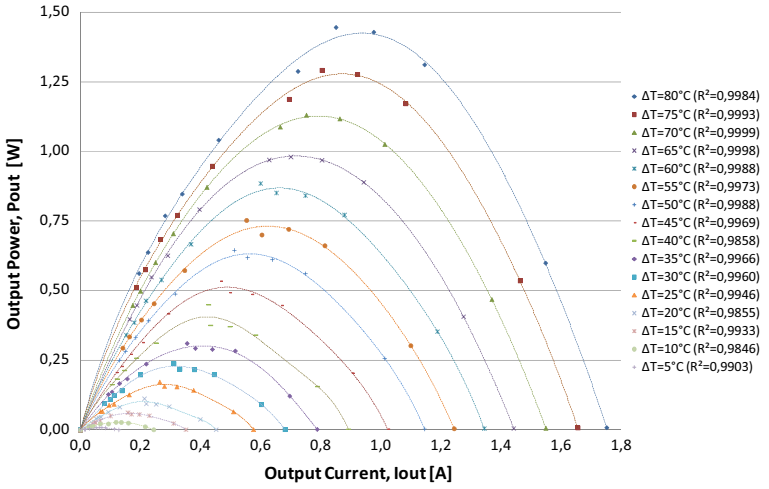


**Fig. 15.** The output power, $P_{out}$ [V] versus the output current, $I_{out}$ [A], for different temperature gradient, $\Delta T$ [°C].

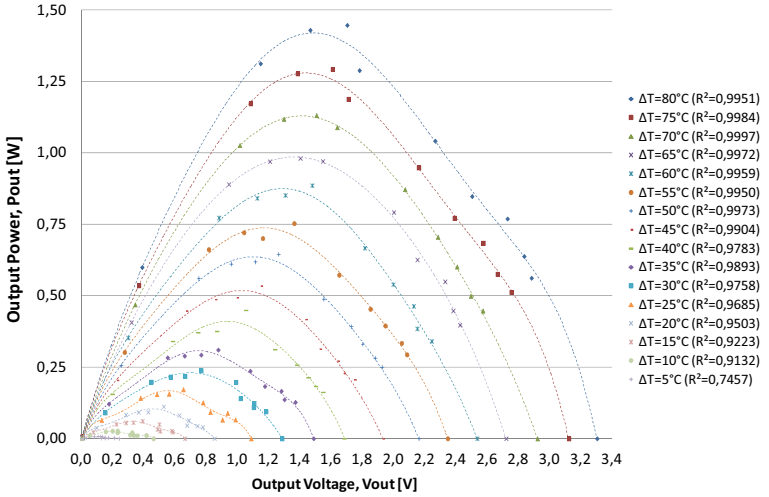


**Fig. 16.** The output power, $P_{out}$ [V] versus the output voltage, $V_{out}$ [V], for different temperature gradient, $\Delta T$ [°C].

Fig. 13b a dotted line represents the trend line of the average internal resistance and its standard deviation ($\pm\sigma$), demonstrating that the internal resistance ($R_{int}$) has a linear variation trend line with the increase of the gradient of temperature ($\Delta T$).

While the last bar to the right of the graph labeled "$R_{int\_average}$" is the average of the resistance values. The average internal resistance ($R_{int\_média}$) of the samples are represented by triangles ($R_{int\_média} = [\mu_1 + \mu_2 + \mu_3 + \mu_4\ \mu_5 + \mu_6 + \mu_7 + \mu_8 + \mu_9 + \mu_{10} + \mu_{11} + \mu_{12} + \mu_{13} + \mu_{14} + \mu_{15} + \mu_{16}]/16 = 1.88\ \Omega$), while the circle symbol indicates the standard deviation of the sample set ($\sigma_{médio} = \sigma_1 + \sigma_2 + \sigma_3 + \sigma_4 + \sigma_5 + \sigma_6 + \sigma_7 + \sigma_8 + \sigma_9 + \sigma_{10} + \sigma_{11} + \sigma_{12} + \sigma_{13} + \sigma_{14} + \sigma_{15} + \sigma_{16} = 0.155\ \Omega$) and are equidistant from the center marked by t he triangle ($R_{int\_average}$). Consequently, it is clear that the internal resistance ($R_{int\_average}$) analyzed of the association of modules is equal to $R_{int\_average} = 1.88\ \Omega$ with a tolerance equal to $\Delta R_{int\_average} = 0.155\ \Omega$, in other words, $R_{int} = R_{int} \pm R_{int\_average} = 1.88 \pm 0.155\ \Omega$. When testing with fixed charges (see Fig. 14) to different temperature gradients ($\Delta T = TH–TL$ [°C]), it's possible to see that, similarly.

Their output voltage ($V_{out}$) and the output current ($I_{out}$) increases in direct proportion to the increased temperature gradient ($\Delta T$), that is, an increase in the output power ($P_{out}$). It is also observed linearity between the curves for different temperature gradients ($DT = TH–TL$ [°C]). This is because the internal resistance ($R_{int}$) of the thermoelectric module has a linear behavior as a function of test temperature gradient. Analyzing the data it can be seen that an increase in the temperature gradient ($DT$) will provided a proportionally power increase ($P_{out}$) in [W] for a given fixed load, $RL$ in [Ω], in other words, the load power will be $P_{out} = RL \cdot I_{out2}$ [W]. Based on this and using different resistance values, as fixed load $RL$ [Ω], it is possible to obtain the maximum power curve graph provided ($P_{out}$) in [W], as function of the output current ($I_{out}$) [A] shown in Fig. 13, for different temperature gradients ($\Delta T$). Additionally, the maximum power curve graph provided ($P_{out}$) [W] according to the output voltage ($V_{out}$) [V] is shown in Fig. 14 for different temperature gradients ($\Delta T$).

Through the power curve analysis provided ($P_{out}$) [W], shown in Figs. 15 and 16, it is possible to determine the maximum power supplied on the basis of the output voltage ($V_{out}$) and output current ($I_{out}$) of the combination of modules in series for different temperature gradients ($\Delta T$).

## 5. Conclusions

Using an acquisition system, calibrated and linearized, the curves were obtained with low error, of around ±1.5%. In addition the precise temperature control was achieved, using PID control tools, with error of only ±2 °C. Another advantage is the ability to export data to spreadsheets, which allows better use of information acquired.

While the association of the modules characterization tests were performed to validate the proposed system, demonstrating consistent with the data presented in [11,6]. The inbC1-127.08HTS module Thermoelectric Power Generation is capable of supplying an output power ($P_{out} = 1.4474$ W) providing an output current (Isaída = 850.55 mA) and an output voltage ($V_{out} = 1.701$ V). The resistance of 1.99 Ω ($V_{out}/I_{out}$) is also consistent with the measurements because it is located in the interval $[\mu - \sigma, \mu + \sigma]\ \Omega$, where $R_0 = 1.88\ \Omega$ and $\sigma = \Delta R_{int} = 0.155\ \Omega$.

Finally, we highlight that the acquisition and monitoring system for characterization of TEG was effective and combined with its low installation cost (about R$973.80 or ≈324.43 €) becomes a viable alternative for use as a laboratory tool or didactic equipment for a wide range of applications where it is desirable TEG characterization.

## References

[1] O.H. Ando Junior, J.A.H. Haffner, O setor elétrico como ferramenta estratégica de gestão governamental, CAESURA: Revista Crítica de Ciências Sociais e Humanas, Canoas, v. 34. Jun. 2009, pp. 121–142 (Semestral).
[2] A. Vargas-Almeida, M.A. Olivares-Robles, P. Camacho-Medina, Thermoelectric system in different thermal and electrical configurations: its impact in the figure of merit, Entropy 15 (2013) 2162–2180.
[3] N. Smith, R. McCann, Investigation of a multiple input converter for grid connected thermoelectric-photovoltaic hybrid system, in: Green Technologies Conference, 19–20 April 2012, IEEE, 2012, pp. 15. <http://dx.doi.org/10.1109/GREEN.2012.6200938>.
[4] R. Singh, N. Gupta, K.F. Poole, Global green energy conversion revolution in 21st century through solid state devices, in: 26th International Conference on Microelectronics 2008, MIEL 2008, 11–14 May 2008, pp. 45–54. <http://dx.doi.org/10.1109/ICMEL.2008.4559221>.
[5] S. Karabetoglu, A. Sisman, Characterization of a thermoelectric generator at low temperatures, Energy Convers. Manage. 62 (April) (2012) 47–50.
[6] O.H. Ando Junior et al., Proposal of a thermoelectric microgenerator based on seebeck effect to energy harvesting in industrial processes, Renew. Energy Power Qual. J. (RE&PQJ) 1 (2014) 227–333.
[7] S. Maharaj, P. Govender, Waste energy harvesting with a thermoelectric generator, in: Proceedings of the 21st Domestic Use of Energy Conference (DUE), vol., no., 3–4 April 2013, pp. 1–6.
[8] P. Camacho-Medina, M.A. Olivares-Robles, A. Vargas-Almeida, F. Solorio-Ordaz, Maximum power of thermally and electrically coupled thermoelectric generators, Entropy 16 (5) (2014) 2890–2903.
[9] Kim Bunthern, Bun Long, et al., Modeling and tuning of MPPT controllers for a thermoelectric generator, in: First International Conference on Green Energy, 2014, pp. 220–226.
[10] O.H. Ando Junior, C.L. Izidoro, J.M. Gomes, J.H. Correia, J.P. Carmo, L. Schaeffer, Acquisition and monitoring system for TEG characterization, Int. J. Distrib. Sens. N. 2015 (2015) 7, http://dx.doi.org/10.1155/2015/531516 531516.
[11] J.P. Carmo et al., Characterization of thermoelectric generators by measuring the load-dependence behavior, Measurement 44 (10) (2011) 2194–2199, http://dx.doi.org/10.1016/j.measurement.2011.07.015.